PRAMANA — journal of physics
© Indian Academy of Sciences
Vol. 72, No. 6
June 2009
pp. 939–950

Evolution of optical pulses in the presence of third-order dispersion

DEBABRATA PAL, Sk GOLAM ALI and B TALUKDAR*
Department of Physics, Visva-Bharati University, Santiniketan 731 235, India
*Corresponding author. E-mail: binoy123@bsnl.in

MS received 26 September 2008; revised 19 March 2009; accepted 1 May 2009

Abstract. We model the propagation of femtosecond pulses through optical fibres by a nonlinear Schrödinger (NLS) equation involving a perturbing term arising due to third-order dispersion in the medium. The perturbative effect of this higher-order dispersion causes the usual NLS soliton to emit a radiation field. As a result, the given initial pulse propagating through the fibre exhibits nonsolitonic behaviour. We make use of a variational method to demonstrate how an initial pulse by the interaction with the emitted radiation can evolve into a soliton. We also demonstrate that the effect of interaction between the initial pulse and radiation field can be accounted for by including, in the evolution equation, terms associated with self-steepening and stimulated Raman scattering that characterize the optical medium.

Keywords. Femtosecond optical pulses; nonlinear media; third-order dispersion; self-steepening; stimulated Raman scattering.

PACS Nos 42.81.Dp; 03.40.Kf; 42.65.Tg; 42.79.Sz

1. Introduction

The propagation of picosecond pulses through optical fibres is well described by the nonlinear Schrödinger (NLS) equation

$$i\phi_x + \phi_{tt} + |\phi|^2\phi = 0 \tag{1}$$

with $\phi = \phi(x,t)$, a complex wave field. Here t stands for time and x is the coordinate along the direction of propagation. The suffixes x and t of ϕ denote partial derivatives with respect to these variables. In particular, $\phi_{tt} = \partial^2\phi/\partial t^2$. An interplay between the self-phase modulation ($|\phi|^2\phi$) and second-order group velocity dispersion (ϕ_{tt}) produces the so-called optical soliton which propagates without changes in its parameter values and without emitting any radiation. However, there exists physical processes, like the propagation of femtosecond pulses, which lead to the break down of this stationary nature of soliton propagation. One of the processes of this type, which is of special importance for ultra-short pulses is associated with the third-order dispersion [1]. In this case the evolution for pulse propagation is given by

$$i\phi_x + \phi_{tt} + |\phi|^2\phi = i\beta\phi_{ttt}. \tag{2}$$

Numerical simulations have shown that solitonic pulses propagating in the presence of third-order dispersion experience corruption [2]. This appears to be the main reason to have in the literature a detailed theoretical study [3] for solving (2). The third-order dispersion in (2) perturbs the soliton of (1). The parameter β is a measure of this perturbation. The main theoretical method for studying the perturbed soliton dynamics is the so-called 'associated' field formalism based on results from the inverse scattering theory [2]. In the presence of perturbation, the NLS soliton generates a radiation field. As a result, the conserved quantities (infinitely many) associated with the unperturbed equation exhibit spatial variation. This basic assumption is exploited to investigate the soliton dynamics of (2). Our objective in this work is to examine how the interaction between the generated dispersive radiation and initial pulse might produce a stable soliton for certain parameter values characterizing the evolution of the former.

We note that eq. (2) is not physically complete. In addition to the third-order dispersive term we need to consider the effects of self-steepening (SS) and self-frequency shift arising from stimulated Raman scattering (SRS). When these effects are taken into consideration, eq. (2) modifies to

$$i\phi_x + \phi_{tt} + |\phi|^2\phi = i\beta\phi_{ttt} + ic_1(|\phi|^2\phi)_t + ic_2\phi(|\phi|^2)_t, \tag{3}$$

where the second term in the right-hand side accounts for self-steepening while the third term is associated with the effect of Raman scattering. Here c_1 and c_2 are real parameters related to SS and SRS respectively. It is interesting to note that while (2) is nonintegrable, a coupled amplitude-phase formulation [4] can be used to solve (3) analytically. More significantly, this formulation has been adapted by Li *et al* [5] to obtain new types of solitary wave solutions for higher-order nonlinear Schrödinger equation.

For femtosecond pulses the effect of third-order dispersion is significant if the group velocity dispersion is close to zero. Otherwise ϕ_{ttt} can be neglected from the evolution equation in (3). In the latter case the effects of SS and SRS, however, remain dominant and one needs to retain only the second and third terms in the right side of (3). In the recent past, Vyas *et al* [6] found exact solutions for the nonlinear Schrödinger equation in the presence of self-steepening and frequency shift induced by SRS. Admittedly, the known expressions in refs [4,6] provide a basis to make some useful checks on the results obtained by considering the interaction between the dispersive radiation and initial pulse because these expressions are expected to give exact results for soliton profiles. As an added realism we shall, therefore, compare our results as obtained from (2) by considering the interaction between the initial pulse and emitted radiation field with those computed from (3) for cases where (i) all three terms on the right side are present and (ii) only the third-order term is absent. A purely numerical routine, namely, the Crank–Nicholson method [7] can be employed to obtain numbers for profile values as accurate as those given by the analytic expressions of Palacios *et al* and Vyas *et* *al*. Thus, it appears rather flexible to numerically simulate the influence of SS and SRS on the pulse propagation.

In §2 we convert (2) into a variational problem and find an expression for the associated Lagrangian density which in conjunction with a suitably chosen trial function defines a reduced variational problem [8]. The reduced variational problem thus obtained via Ritz optimization procedure [9] helps us to construct coupled differential equations for the parameters of the trial function. In §3 we study how, for (2), initial pulses evolve into solitons. For equations of the parameters there is a fixed point at which initial pulses always form solitons. As one goes away from the fixed point, the initial pulses propagate as solitary waves and subsequently decay. We find that if the effect of radiation loss of the perturbed NLS soliton is included in formulating the variational problem, the initial pulses will evolve into solitons even if we move away from the fixed point. We then compare the results of the third-order NLS equation so obtained with those of the generalized higher-order equation in (3). We separately consider cases where all three higher-order terms are present [4] and where only the dispersive effect due to ϕ_{ttt} is absent [6]. The comparison made by us reveals that while the third-order dispersion tends to destabilize the initial pulse by inducing nonsolitonic behaviour, the self-steepening and self-frequency shift due to stimulated Raman scattering do the opposite such that the initial pulse could propagate as a soliton. In the absence of third-order dispersion, the nonsolitonic behaviour disappears. In this case the effects of SS and SRS manifest themselves in producing a more energetic soliton than that found from the NLS equation in (1). In §4 we make some concluding remarks.

2. Variational formulation of (2)

The initial boundary value problem of third-order NLS equation can be obtained from the action principle

$$\delta \int\int \mathcal{L}\left(\phi,\, \phi^*,\, \phi_t,\, \phi_t^*,\, \phi_{2t},\, \phi_{2t}^*,\, \phi_x,\, \phi_x^*\right) \mathrm{d}x\, \mathrm{d}t = 0 \tag{4}$$

with the Lagrangian density given by

$$\mathcal{L} = \frac{i}{2}\left(\phi\phi_x^* - \phi^*\phi_x\right) - \frac{1}{2}\phi^2\phi^{*2} + \phi_t\phi_t^* + \frac{i\beta}{2}\left(\phi_t\phi_{2t}^* - \phi_t^*\phi_{2t}\right). \tag{5}$$

To study the effect of dispersive radiation associated with the term ϕ_{ttt} on the soliton solution of (1) we note that for the NLS equation there exists a well-defined spectral problem [10] such that one can write a closed form analytical solution of it in terms of 'sech' functions. As opposed to this, the third-order equation (2) is nonintegrable and cannot be solved analytically. Nevertheless, we assume the solution of (2) to have the same analytic form as that of (1) but with space-dependent soliton parameters. We thus introduce a function

$$\phi(x,t) = \left[\eta(x)\,\mathrm{sech}\left(\frac{t-y(x)}{a(x)}\right) + ig(x)\right] \exp i\left[V(x)(t-y(x)) + \sigma(x)\right] \tag{6}$$

for a trial solution of the third-order NLS equation. Here the parameters η, y and a are related to the three lowest-order moments of the ϕ envelope and represent its amplitude, central position and width respectively. The other parameters σ and V stand for the phase and velocity (centre of the soliton) respectively. The parameter g is a representative for the low-frequency radiation emitted by NLS soliton due to the effect of perturbation. This radiation does not propagate away but forms a flat shelf under the decaying NLS soliton [11]. We shall investigate how the interaction between the shelf and decaying wave ultimately produces a stable soliton. Inserting the trial function (6) into the variational principle in (4) we obtain the reduced variational problem

$$\delta \int \langle \mathcal{L} \rangle \, \mathrm{d}x = 0 \tag{7}$$

with

$$\langle \mathcal{L} \rangle = \int_{\infty}^{\infty} \mathcal{L}_s \, \mathrm{d}t. \tag{8}$$

Here $\mathcal{L}_s$ denotes the result of inserting 'sech' ansatz into the Lagrangian density $\mathcal{L}$. By performing the integration in (8) we obtain

$$\begin{aligned}\langle \mathcal{L} \rangle = & -2a\eta^2 V \frac{\mathrm{d}y}{\mathrm{d}x} + 2a\eta^2 \frac{\mathrm{d}\sigma}{\mathrm{d}x} + \pi a\eta \frac{\mathrm{d}g}{\mathrm{d}x} - \pi\eta g \frac{\mathrm{d}a}{\mathrm{d}x} - \pi g a \frac{\mathrm{d}\eta}{\mathrm{d}x} - g^2 y l \frac{\mathrm{d}V}{\mathrm{d}x} \\ & -g^2 l V \frac{\mathrm{d}y}{\mathrm{d}x} + g^2 l \frac{\mathrm{d}\sigma}{\mathrm{d}x} - \frac{2}{3} a\eta^4 - 2a\eta^2 g^2 + \frac{2\eta^2}{3a} + g^2 V^2 l + 2a\eta^2 V^2 \\ & +2\frac{\beta V \eta^2}{a} + g^2 \beta V^3 l + 2a\beta\eta^2 V^3. \end{aligned} \tag{9}$$

The occurrence of the unknown factor l in (9) needs some clarification. Physically, the first term inside the square bracket of (6) represents a varying soliton-like pulse and allows the initial data to evolve smoothly into a soliton solution. It includes the variational parameters η and a arising due to in-phase interaction of the unperturbed soliton with the shelf. In contrast, the second term g represents the out-of-phase interaction between the soliton and shelf. This term can be assumed to be independent of t in the vicinity of the soliton such that g contributes to the Lagrangian only in a region of length l centred about the pulse position [11]. In fact the length l entered into (9) from the replacement of integrals like $\int_{-\infty}^{\infty} g^2 V (\mathrm{d}y/\mathrm{d}x)\mathrm{d}t$ by $\int_{-l/2}^{l/2} g^2 V (\mathrm{d}y/\mathrm{d}x)\mathrm{d}t$. Understandably, the terms proportional to l give the amount of mass for the radiation in the vicinity of the pulse. We shall see that the length parameter l can be expressed in terms of $\eta(0)$, $a(0)$, V and β from some physical requirements about the linearized solution of (2). Meanwhile, let us proceed to study the variational equations for the parameters in the trial function on the basis of (7). From the vanishing conditions [9] of variationals like $\delta\langle \mathcal{L} \rangle/\delta\sigma$, $\delta\langle \mathcal{L} \rangle/\delta a$, $\delta\langle \mathcal{L} \rangle/\delta y$, $\delta\langle \mathcal{L} \rangle/\delta\eta$, $\delta\langle \mathcal{L} \rangle/\delta V$ and $\delta\langle \mathcal{L} \rangle/\delta g$ we obtain the following equations:

$$\frac{\mathrm{d}}{\mathrm{d}x} \left(2a\eta^2 + l g^2 \right) = 0, \tag{10}$$

$$\pi \frac{\mathrm{d}}{\mathrm{d}x}(g\eta) = 2\eta^2 V \frac{\mathrm{d}y}{\mathrm{d}x} - 2\eta^2 \frac{\mathrm{d}\sigma}{\mathrm{d}x} - \pi\eta \frac{\mathrm{d}g}{\mathrm{d}x} + \pi g \frac{\mathrm{d}\eta}{\mathrm{d}x} + \frac{2}{3}\eta^4 + \frac{2}{3}\frac{\eta^2}{a^2} \\ -2\eta^2 V^2 + \frac{2\beta V \eta^2}{a^2} - 2\beta\eta^2 V^3, \tag{11}$$

$$\frac{\mathrm{d}}{\mathrm{d}x}\left(2a\eta^2 V + g^2 l V\right) = g^2 l \frac{\mathrm{d}V}{\mathrm{d}x}, \tag{12}$$

$$\pi \frac{\mathrm{d}}{\mathrm{d}x}(ag) = 4a\eta V \frac{\mathrm{d}y}{\mathrm{d}x} - 4a\eta \frac{\mathrm{d}\sigma}{\mathrm{d}x} - \pi a \frac{\mathrm{d}g}{\mathrm{d}x} + \pi g \frac{\mathrm{d}a}{\mathrm{d}x} + \frac{8}{3}a\eta^3 - \frac{4\eta}{3a} \\ -4a\eta V^2 - \frac{4\beta V \eta}{a} - 4a\beta\eta V^3, \tag{13}$$

$$2a\eta^2 \frac{\mathrm{d}y}{\mathrm{d}x} + g^2 l \frac{\mathrm{d}y}{\mathrm{d}x} - 2g^2 l V - 4a\eta^2 V - \frac{2\beta\eta^2}{a} - 3g^2\beta V^2 l - 6a\beta\eta^2 V^2 = 0, \tag{14}$$

and

$$\pi \frac{\mathrm{d}}{\mathrm{d}x}(a\eta) = -\pi a \frac{\mathrm{d}\eta}{\mathrm{d}x} - \pi\eta \frac{\mathrm{d}a}{\mathrm{d}x} - 2gVl \frac{\mathrm{d}V}{\mathrm{d}x} - 2glV \frac{\mathrm{d}y}{\mathrm{d}x} + 2gl \frac{\mathrm{d}\sigma}{\mathrm{d}x} + 2gV^2 l. \tag{15}$$

In writing (10)–(15) we assumed $g^2 l \gg g^2$. Also we neglected all terms involving g^n when $n \geq 3$. We can combine (10) and (12) to get

$$V = \text{constant}. \tag{16}$$

At the same time eqs (11), (13)–(16) lead to the evolution equations

$$\frac{\mathrm{d}a}{\mathrm{d}x} = \frac{lg}{3\pi\eta}\left(4\eta^2 - \frac{2(1+3\beta V)}{a^2}\right), \tag{17}$$

$$\frac{\mathrm{d}\eta}{\mathrm{d}x} = -\frac{lg}{\pi a}\left(\frac{\eta^2}{3} + \frac{(1+3\beta V)}{3a^2}\right), \tag{18}$$

$$\frac{\mathrm{d}y}{\mathrm{d}x} = 2V + 3\beta V^2 + \frac{\beta}{a^2} + \frac{g^2 l V}{a\eta^2} + \frac{3}{2}\frac{g^2\beta V^2 l}{a\eta^2} \\ + \frac{2gyl}{\pi a\eta}\left(-\frac{\eta^2}{3} + \frac{2}{3a^2} + \frac{2\beta V}{a^2}\right) \tag{19}$$

and

$$\frac{\mathrm{d}g}{\mathrm{d}x} = -\frac{2}{3\pi}\left(\eta^3 - \frac{2(1+3\beta V)\eta}{a^2}\right) \tag{20}$$

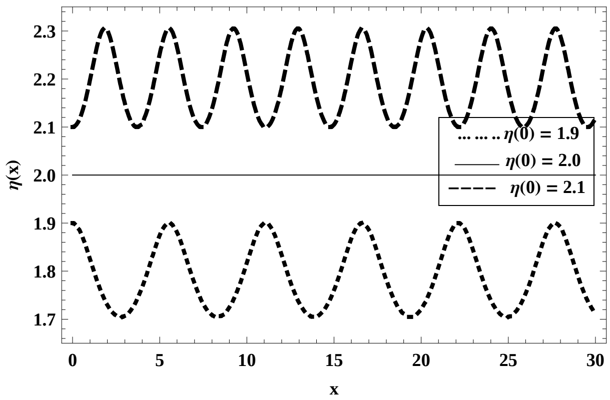

Figure 1. $\eta(x)$ as a function of x for three different values of $\eta(0)$.

for $a(x)$, $\eta(x)$, $y(x)$ and $g(x)$. From (20) it is evident that the system of coupled equations from (17) to (20) have a fixed point at

$$\eta = \frac{\sqrt{2(1+3\beta V)}}{a} \tag{21}$$

giving the condition for the existence of a soliton solution for the third-order NLS equation. The length l is determined by the requirement that the frequency of oscillations of the linearized solution of (2) about this critical point is equal to the soliton oscillation frequency. This gives [11,12]

$$l = \frac{3\pi^2}{8k} \tag{22}$$

with

$$k^3 = a\eta^4 - \frac{\eta^2(1+3\beta V)}{a}, \tag{23}$$

the soliton energy.

3. Results for evolution of initial pulses

To study the evolution of the initial pulse in the presence of third-order dispersion we solved the set of coupled equations from (17)–(20) with initial conditions $a(0) = 1$, $y(0) = 0$ and $g(0) = 0$. The solutions were obtained for three different values of $\eta(0)$. First we took $\eta(0)\,(= \eta_f(0) = 2)$. This value corresponds to an initial condition for $\eta(x)$ determined from the fixed point (21) of these equations for $\beta V = 1/3$. For the other two initial values we decided to work with $\eta(0) = \eta_f(0) \pm 0.1$.

In figure 1 we plot $\eta(x)$ as a function of x. The curve for the initial condition $\eta_f(0) = 2$ is a straight line (solid curve) parallel to the x-axis. This implies that at the fixed point of (17)–(20), the amplitude of the soliton as a function of x remains

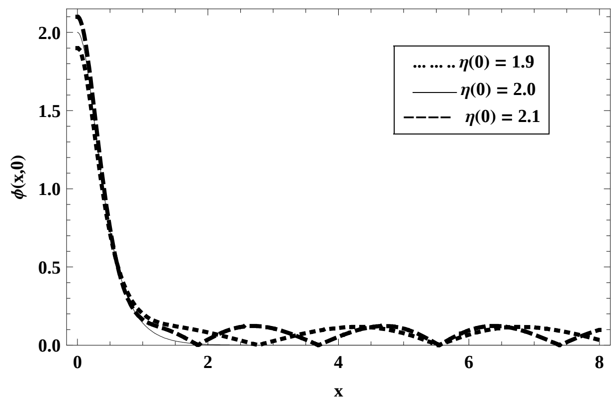

Figure 2. The absolute value of the optical pulse $|\phi(x,0)|$ as a function of x for the same values of $\eta(0)$ as in figure 1.

constant. The other two curves for $\eta(0) = 2.1$ (dashed curve) and $\eta(0) = 1.9$ (dotted curve) exhibit oscillatory behaviour. In figure 2 we plot $|\phi(x,0)|$ as a function of x for the same set of values of $\eta(0)$ as used in the plot of $\eta(x)$. Looking closely into this figure we see that the curves of $|\phi(x,0)|$ for $\eta(0) = 1.9$ (dotted curve) and $\eta(0) = 2.1$ (dashed curve) have oscillatory tails. On the other hand, no such oscillations on the tail appear in the curve of $|\phi(x,0)|$ for $\eta_f(0) = 2$ (solid curve). Thus, only for $\eta(0)$ determined from the fixed point of (17)–(20) the initial pulse propagates as a soliton. But as we go away from $\eta_f(0) = 2$ to choose the value of $\eta(0)$ we get nonsolitonic solutions of (2) characterized by the presence of oscillatory tails. This happens because we did not include contribution from the radiation propagating away from the vicinity of the pulse. In the following we show that by taking appropriate care of this radiation loss we can construct soliton solutions even for $\eta(0) \neq \eta_f(0)$. Understandably, such solitons will represent embedded solitons.

The detailed radiation analysis carried out in ref. [11] showed that when radiation loss is added the equation of g is modified as

$$\frac{\mathrm{d}g}{\mathrm{d}x} = -\frac{2}{3\pi}\left(\eta^3 - \frac{2(1+3\beta V)}{a^2}\right) - 2\alpha g, \tag{24}$$

where the loss coefficient

$$\alpha = \frac{3k}{8}\frac{r(x)}{r(0)\sqrt{\pi x}} \tag{25}$$

with $r(0)$ given by

$$r^2(x) = \frac{3k}{8}(2a\eta^2 - 2k + lg^2). \tag{26}$$

The variable r measures the difference between the mass of the pulse plus its associated shelf and the steady state mass of the pulse [12]. The modification sought for the g equation causes appropriate changes in other modulation equations for the soliton parameters such that (17), (18) and (19) now read

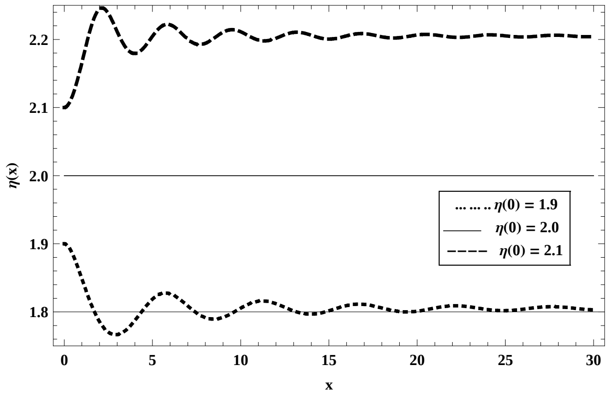

Figure 3. Same as figure 1 but with radiation loss included.

$$\frac{\mathrm{d}a}{\mathrm{d}x} = \frac{lg}{3\pi\eta}\left(4\eta^2 - \frac{2(1+3\beta V)}{a^2}\right) - \frac{2\alpha l g^2}{\eta^2}, \tag{27}$$

$$\frac{\mathrm{d}\eta}{\mathrm{d}x} = -\frac{lg}{\pi a}\left(\frac{\eta^2}{3} + \frac{1+3\beta V}{3a^2}\right) + \frac{2\alpha l g^2}{a\eta} \tag{28}$$

and

$$\frac{\mathrm{d}y}{\mathrm{d}x} = 2V + 3\beta V^2 + \frac{\beta}{a^2} + \frac{g^2 lV}{a\eta^2} + \frac{3g^2\beta V^2 l}{2a\eta^2} + \frac{2gyl}{\pi a\eta}\left(-\frac{\eta^2}{3} + \frac{2}{3a^2} + \frac{2\beta V}{a^2} - \frac{\pi\alpha g}{\eta}\right). \tag{29}$$

To examine how the proper inclusion of the radiation loss affects the evolution of the initial pulse we solved the coupled equations given by (24), (27)–(29) with the same initial conditions as used for eqs (17)–(20). Figure 3 gives the plot of $\eta(x)$ as a function of x. As before, the solid curve for $\eta_f(0) = 2$ is a straight line. The other two curves, however, exhibit entirely different behaviour when compared to that of the corresponding curves in figure 1. For example, rather than showing oscillatory behaviour with constant amplitude, the initial oscillations in both curves for $\eta(0) = 2.1$ (dashed curves) and $\eta(0) = 1.9$ (dotted curve) damp out leading to constant amplitudes. This implies that we have soliton solutions even if we are away from the fixed point and this has been possible by taking appropriate care of the radiation loss. In figure 4 we plot $|\phi(x, 0)|$ as a function of x for $\eta_f(0) = 2$ (solid curve), $\eta(0) = 2.1$ (dashed curve) and $\eta(0) = 1.9$ (dotted curve). As with the curve for $\eta_f(0) = 2$, the other two curves for $\eta(0) = 2.1$ and $\eta(0) = 1.9$ are free from oscillatory tails showing explicitly that we can now have soliton solutions of (2) even for $\eta(0) \neq \eta_f(0)$.

We noted that compared to (2), eq. (3) models the propagation of femtosecond pulses through optical fibres more realistically. Equation (3) has been solved analytically such that (11) in ref. [4] can be integrated under appropriate conditions

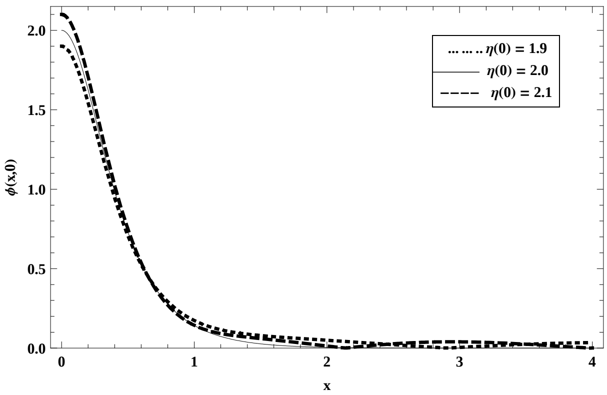

Figure 4. Same as figure 2 but with radiation loss included.

to obtain bright optical solitary wave solutions. Similar analytical solution of (3) in the absence of the ϕ_{ttt} term have been given by Vyas *et al* [6] taking recourse to the use of a conformal Möbius transformation. We shall now exploit the findings of these works to examine the results presented in figures 2 and 4. We are particularly interested to see how the nonsolitonic behaviour for the solution of (2) is remedied by the SS and SRS terms in (3). For that we first numerically simulated the results of profile values as given by the expressions of Palacios *et al* [4] and Vyas *et al* [6] by using Crank–Nicholson method [7].

To solve partial differential equations numerically one first replaces the partial derivatives involved by the corresponding difference quotients and subsequently solves the set of simultaneous equations associated with appropriate initial and boundary conditions. For a typical evolution equation written in the usual notation, the time derivative is represented as a forward difference since we do not have any information for negative time at the start [13]. The space derivatives are, however, written using central differences. The difference equation thus obtained is often called the 'explicit form' of discrete representation of the given equation. It is numerically unstable if the time step of discretization is not extremely small. This puts severe restrictions on the usefulness of the 'explicit form' for integrating partial differential equations. The 'implicit form' of discretization provided by the Crank–Nicholson method imposes no restriction on time and space step sizes. This motivated us to work with the method of Crank and Nicholson. To preserve normalization of the solutions, the implicit method needs to be supplemented by the Cayley form of the unitary operator [14] that enters into the formulation. We modified the original Crank–Nicholson algorithms by interchanging x and t for application to equations written in the optical notation and then solved (2) and (3) with initial and boundary conditions $\phi(t,0) = \mathrm{sech}(t)\mathrm{e}^{i\pi t}$, $\phi(-25,x) = \phi(25,x)$ and $\phi_x(-25,x) = \phi_x(25,x)$. Note that the second boundary condition is not necessary to solve NLS equation (1).

We present in figure 5 curves for $|\phi_3(x,0)|$ and $|\phi_f(x,0)|$ as a function of x. The subscripts 3 and f of ϕ refer to solutions of the third-order equation (2) and full equation in (3). As expected, the curve (dotted) for $|\phi_3(x,0)|$ has an oscillatory

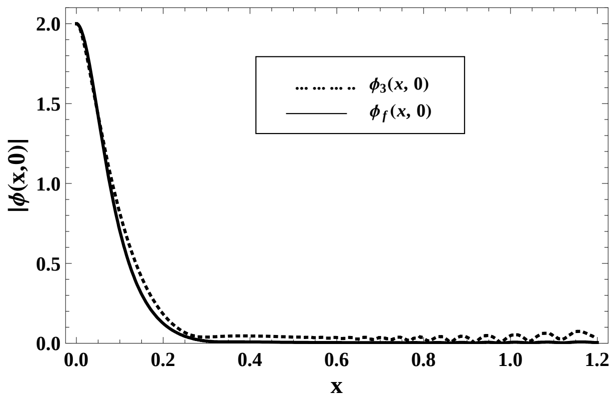

Figure 5. Absolute values of optical pulses ($|\phi(x,0)|$) vs. x as computed from (2) and (3).

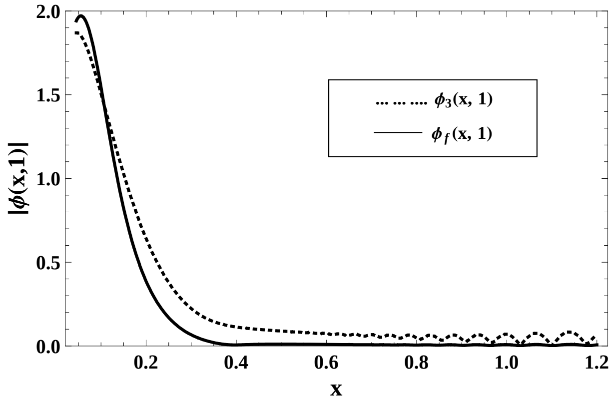

Figure 6. Same as figure 5 but with pulse values calculated for $t = 1$.

tail associated with the nonsolitonic behaviour of the solitary wave solution of (2). The curve (solid) for $|\phi_f(x,0)|$ clearly shows that oscillations on the tail have disappeared due to inclusion of the effects arising from SS and SRS terms with $c_1 = -2.5$, $c_2 = 2.5$ and $\beta = 0.5$. But in figure 4 we found that the oscillatory tail vanishes due to interaction of the NLS soliton with the emitted radiation field. Thus the postulated soliton-radiation-field interaction as used by us to stabilize the solitary wave solution of the third-order NLS equation appears to have its physical origin in the self-steepening and self-frequency shift arising from SRS. We portray in figure 6 curves similar to those in figure 5 but with $t = 1$. Clearly, the spatial behaviour of $|\phi_3(x,1)|$ and $|\phi_f(x,1)|$ is identical to that found for $|\phi_3(x,0)|$ and $|\phi_f(x,0)|$ except that the peak value of $|\phi_f(x,1)|$ is slightly augmented and shifts slightly to the right when compared with the peak value of $|\phi_f(x,0)|$. In figure 7 we plot $|\phi_2(x,0)|$ (dotted curve) and $|\phi_{f'}(x,0)|$ (solid curve) against x. Here $\phi_2(x,0)$ represents the soliton solution of the NLS equation while $\phi_{f'}(x,0)$ is the solution of (3) in the absence of the term ϕ_{ttt}. The two curves are almost overlapping indicating

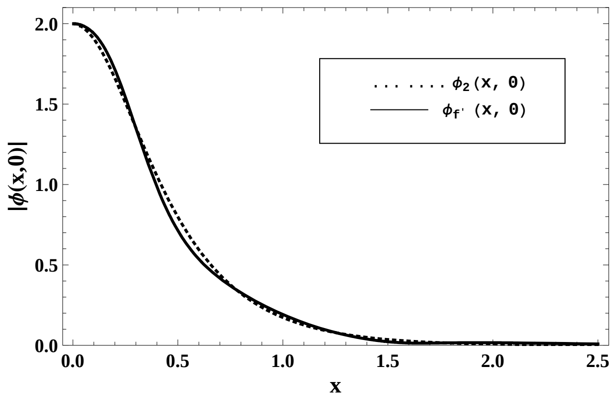

Figure 7. Modulus of profile values ($|\phi(x,0)|$) as a function of x for the NLS equation and for (3) in the absence of third-order dispersion term.

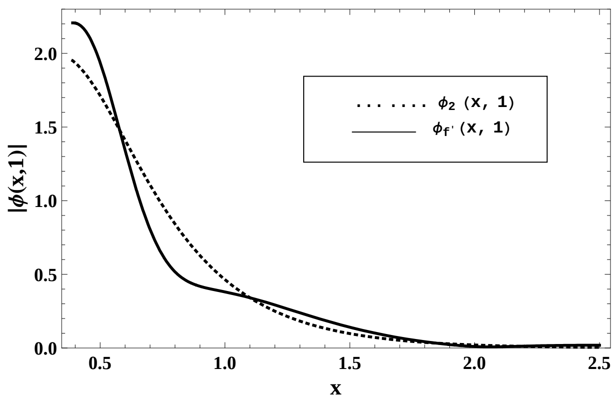

Figure 8. Same as figure 6 but with pulse values calculated for $t = 1$.

that the effects of self-steepening and Raman scattering are not very prominent for $t = 0$. Figure 8 gives similar curves for $t = 1$. Looking into this figure we see that for $x < 2$ the values of $|\phi_{f'}(x,1)|$ deviate considerably from the profile values of the NLS soliton. In particular, we find that $|\phi_{f'}(x,1)|_{x=0} > |\phi_2(x,1)|_{x=0}$. Thus, in the present case the effects of SS and SRS tend to produce more energetic soliton.

4. Conclusions

The femtosecond pulses while propagating through an optical fibre tends to lose energy due to perturbation caused by third-order dispersive effects in the medium. A widely used theoretical framework for studying the perturbed soliton dynamics is provided by the 'associated' field formalism derived from some well-known results of the inverse scattering theory [2]. In this work we deal with a variational formulation of the third-order nonlinear Schrödinger equation and make use of a 'sech' trial function to show that an initial pulse can evolve into a soliton despite the perturbing effect of the third-order dispersion. The merit of our approach is that it is, on the one hand, physically transparent, and on the other hand, mathematically uncomplicated. Numerical simulation of our variational results in terms of a generalized third-order NLS equation clearly indicates that self-steepening and frequency-shift due to SRS represent two physical effects that can be manipulated to have solitonic propagation of femtosecond pulses through optical fibres. It, however, remains an interesting curiosity to examine why the numerical and variational solutions of (2) differ in frequency of oscillation on the tail.

Acknowledgement

This work forms the part of a Research Project F.No. 32-39/2006(SR) supported by the University Grants Commission, Govt. of India. One of the authors (SGA) is thankful to the UGC, Govt. of India for a Research Fellowship.

References

[1] G P Agrawal, *Nonlinear fiber optics*, 3rd Edition (Academic Press, San Diego, California, USA, 1995)
[2] J N Elgin, T Brabec and S M J Kelly, *Opt. Commun.* **114**, 3218 (1995)
[3] A Peleg and Y Chung, *J. Phys. A: Math. Gen.* **36**, 10039 (2003)
[4] S L Palacios, A Guinea, J M Fernandez-Diaz and R D Crespo, *Phys. Rev.* **E60**, R45 (1999)
[5] Z Li, Lu Li, H Tian and G Zhou, *Phys. Rev. Lett.* **84**, 4096 (2000)
[6] V M Vyas, P Patel, P K Panigrahi, C N Kumar and W Greiner, *Phys. Rev.* **A78**, 021803(R) (2008)
[7] J Crank and P Nicholson, *Proc. Camb. Phil. Soc.* **43**, 5067 (1947)
[8] D Anderson, *Phys. Rev.* **A27**, 3135 (1983)
[9] G B Arfken and H J Weber, *Mathematical methods for physicists* (Elsevier, New Delhi, 2004)
[10] V E Zakharov and A B Shabat, *Sov. Phys. JETP* **34**, 62 (1972)
[11] A A Minzoni, N F Smyth and A L Worthy, *Physica* **D206**, 16679 (2005)
[12] W L Kath and N F Smith, *Phys. Rev.* **E51**, 1484 (1995)
[13] E Kreyszig, *Advanced engineering mathematics* (New Age International (P) Limited, New Delhi, 1997) ISBN:81-224-0016-1
[14] N Watanabe and M Tsukada, *Phys. Rev.* **E62**, 2914 (2000)